Aalborg Universitet

Comparative Study on Temperature Dependency of dV/dt, dI/dt and EMI Generation for IGBTs, Si and SiC MOSFETs

Davari, Pooya; Xue, Peng

DOI (link to publication from Publisher):
10.1109/EMCEurope61644.2025.11176218

Publication date:
2025

Document Version
Accepted author manuscript, peer reviewed version

Link to publication from Aalborg University

Citation for published version (APA):
Davari, P., & Xue, P. (2025). *Comparative Study on Temperature Dependency of dV/dt, dI/dt and EMI Generation for IGBTs, Si and SiC MOSFETs*. 546-551. Abstract from 2025 International Symposium on Electromagnetic Compatibility (EMC Europe 2025), Paris, France.
https://doi.org/10.1109/EMCEurope61644.2025.11176218

General rights
Copyright and moral rights for the publications made accessible in the public portal are retained by the authors and/or other copyright owners and it is a condition of accessing publications that users recognise and abide by the legal requirements associated with these rights.

- Users may download and print one copy of any publication from the public portal for the purpose of private study or research.
- You may not further distribute the material or use it for any profit-making activity or commercial gain
- You may freely distribute the URL identifying the publication in the public portal -

Take down policy
If you believe that this document breaches copyright please contact us at vbn@aub.aau.dk providing details, and we will remove access to the work immediately and investigate your claim.

Downloaded from vbn.aau.dk on: December 10, 2025

Comparative Study on Temperature Dependency of dV/dt, dI/dt and EMI Generation for IGBTs, Si and SiC MOSFETs

Peng Xue #1, Pooya Davari,#2,

#Department of Energy, Aalborg University, Aalborg East 9220, Denmark

1pexu@energy.aau.dk, 2 pda@energy.aau.dk

***Abstract*—In this paper, a study on the temperature dependency of the dV/dt and dI/dt and electromagnetic interference (EMI) generation is proposed for IGBT, Si MOSFET and SiC MOSFET. During the switching transient, the junction temperature T_{J1} of the low-side switch affects the switching behavior, while the junction temperature T_{J2} of the high-side switch affects turn-on characteristics. The impacts of T_{J1} and T_{J2} are thereby investigated separately to identify their influence on the dV/dt, dI/dt and EMI generation. Based on theoretical analyses and experimental study, the dependencies of the T_{J1} and T_{J2} on dV/dt and dI/dt for IGBT, Si MOSFET and SiC MOSFET are clarified. Using the fast Fourier transform (FFT) on the trapezoidal switching waveforms of the devices, the dependencies of T_{J1} and T_{J2} on the EMI generation are also investigated.**

***Keywords*—temperature dependent, dI/dt, dV/dt, EMI, SiC MOSFET, IGBT, Si MOSFET**

I. Introduction

Nowadays, the temperature dependency of dV/dt, dI/dt and EMI generation of power devices has drawn considerable attention from industry and academia[1], [2], [3], [4], [5]. In [1], [2], [6], the temperature-dependent dV/dt and dI/dt of Si insulated gate bipolar transistor (IGBTs) is studied. Due to the booming of silicon carbide (SiC) MOSFET technology, the temperature dependency of dV/dt and dI/dt and EMI generation for SiC MOSFETs are also investigated in a few papers [4], [5], [7].

The previous studies [1], [2], [3], [4] have some limitations. Firstly, the research mainly focuses on the junction temperature T_{J1} of the low-side active switch. During the switching transient, the junction temperature T_{J2} of the high-side switch can also have a significant impact on the reverse recovery characteristics of its freewheeling diode, which affects the turn-on behavior. The impact of T_{J1} and T_{J2} are thereby needed to be studied separately to identify their temperature dependency on dV/dt and dI/dt. Secondly, the studies mainly focus on a few specific kind of devices. A comparison study on the temperature-dependency of dV/dt and dI/dt for the mainstream power devices like IGBTs, Si and SiC MOSFETs are thereby needed. Last but not least, due to the temperature-dependent dV/dt and dI/dt, the EMI generation also depends on T_{J1} and T_{J2}. However, the related studies receive scarcely attention. The temperature-dependency of EMI generation thereby requires further investigation.

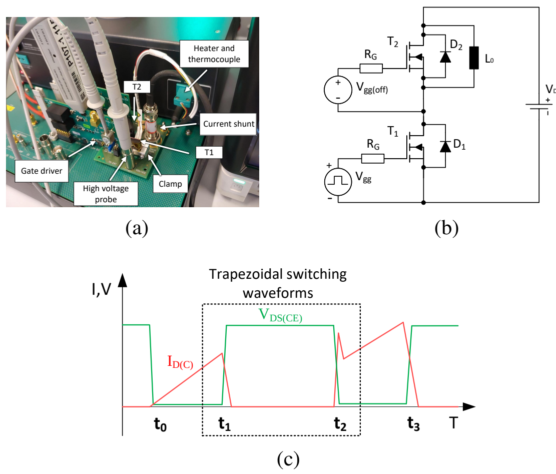

Fig. 1. (a) Double-pulse test fixture. (b) Double-pulse test circuit. (c)Trapezoidal switching waveform obtained form double-pulse test.

In this paper, the temperature dependencies on the dV/dt, dI/dt and EMI generation for the IGBTs I_1 and I_2, Si MOSFETs M_1 and SiC MOSFETs S_1, S_2 and S_3 are extensively investigated using the double-pulse test shown in Fig. 1. The Si MOSFETs M_1 is IXFH60N65X2. The IGBTs I_1 and I_2 are IKW40N65ET7 and IKW40N120C. The SiC MOSFETs S_1, S_2 and S_3 are C3M0045065D, TW048N65C and C2M0080120D. The impact of junction temperature T_{J1} for low-side switch T_1 and junction temperature T_{J2} for high-side switch T_2 on dV/dt, dI/dt are investigated separately. The temperature-dependent parameters and the impact on the dV/dt and dI/dt are investigated theoretically and experimentally for the devices to reveal their T_{J1} and T_{J2} dependencies. The T_{J1} and T_{J2} dependent EMI germination are studied using fast Fourier transform (FFT) on the trapezoidal switching waveforms.

II. Analysis on temperature dependency of dI/dt and dV/dt of IGBTs, Si and SiC MOSFETs

A. T_{J1} dependency of Turn-on dI/dt

The temperature dependency of turn-on $dI/dt|_{on}$ is [8]:

$$\left.\frac{dI^2}{dtdT}\right|_{on} = \frac{\alpha_1 \dfrac{dG_m}{dT} + \beta_1 \dfrac{dV_{th}}{dT}}{\tau_a^2} \tag{1}$$

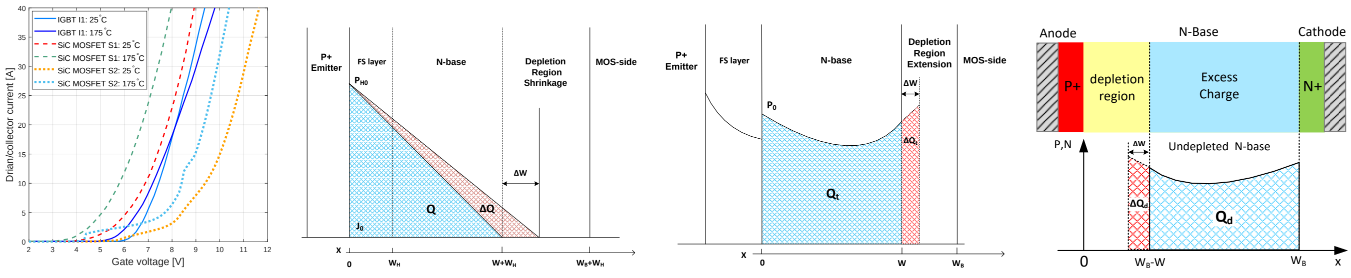

(a) (b) (c) (d)

Fig. 2. (a) IV characteristics of SiC MOSFET and Si IGBT at 25°C and 175°C. (b) Capacitance C_Q at turn-on transient [1]. (c) Capacitance C_{ext} at turn-off transient [2], (d) Charge extraction capacitance C_{ext_d} of bipolar power diode.

where $\alpha_1 = R_G(C_{GS}+C_{GD})(V_{GG(on)}-V_{th})$ and $\beta_1 = -G_m\tau_a$. α_1 is positive while β_1 is negative. As shown in Fig. 2a, SiC MOSFETs have an negative temperature coefficient (NTC) for V_{th}. Its G_m can have a positive temperature coefficient (PTC). The impacts of dV_{th}/dT and dG_m/dT thereby add up, which induces a PTC for the $dI/dt|_{on}$ of SiC MOSFET.

The G_m and V_{th} of IGBTs and Si MOSFETs have NTCs, as shown in Fig. 2a. The impact of dV_{th}/dT and dG_m/dT on $dI^2/dtdT|_{on}$ thereby counteracts. The temperature dependencies on $dI/dt|_{on}$ for the devices are thereby much weaker than that of the SiC MOSFET. Since G_m usually has much stronger temperature dependency, NTCs of $dI/dt|_{on}$ are obtained for IGBTs, Si and SiC MOSFETs.

B. T_{J1} dependency of Turn-off dI/dt

The temperature dependency of turn-off $dI/dt|_{off}$ of IGBT, Si and SiC MOSFETs is [8]:

$$\left.\frac{dI^2}{dtdT}\right|_{off} = \frac{\alpha_2\dfrac{dG_m}{dT} + \beta_2\dfrac{dV_{th}}{dT}}{\tau_a^2} \tag{2}$$

Where $\alpha_2 = R_G(C_{GS}+C_{GD})(V_{th}-V_{GG(off)}) - L_S I_L$ and $\beta_2 = G_m\tau_a$. Noting that β_2 is much larger than α_2 in typical applications, the $dI^2/dtdT|_{off}$ is thereby mainly determined by dV_{th}/dT. Since the IGBT, Si MOSFET and SiC MOSFET have NTCs for V_{th}, their $dI/dt|_{off}$ thereby has a NTC.

C. T_{J1} dependency of Turn-on dV/dt

1) IGBT: Temperature dependency of turn-on dV_{CE}/dt of IGBT is [1]:

$$\left.\frac{dV_{CE}^2}{dtdT}\right|_{on} = \frac{\alpha_3\dfrac{dG_m}{dT} + \beta_3\dfrac{dV_{th}}{dT} + \zeta_3\dfrac{dC_Q}{dT}}{\tau_b^2} \tag{3}$$

$\beta_3 = -G_m\tau_b$. $\zeta_3 = -(G_m(V_{GG(on)}-V_{th}) - I_L)$. $\alpha_3 = (C_Q + C_{CE} + C_{OSS2} + C_{GC})(V_{GG(on)} - V_{th}) + I_L R_G C_{GC}$. $\tau_b = C_Q + C_{CE} + C_{OSS2} + C_{GC}(1+G_m R_G)$. I_L is the load current. C_{OSS2} is the equivalent capacitance of high-side MOSFET. When the depletion region reduces, the excess charge Q increases as shown in Fig. 2b. C_Q is the capacitance generated by the dynamics of N-base excess charge[1].

In the beginning of voltage falling transient, C_Q is approximately temperature independent because high-level injection is not achieved in the N-base [1], which induces a relatively weak temperature dependency on $dV_{CE}/dt|_{on}$. At the end of the turn-on transient when high-level injection conditions is achieved, C_Q is strongly temperature-dependent. This induces the NTC for $dV_{CE}/dt|_{on}$ since ζ_3 is negative.

2) Unipolar devices: Temperature dependency of turn-on dV_{ds}/dt of Si and SiC MOSFETs is:

$$\left.\frac{dV_{DS}^2}{dtdT}\right|_{on} = \frac{\alpha_4\dfrac{dG_m}{dT} + \beta_4\dfrac{dV_{th}}{dT}}{\tau_c^2} \tag{4}$$

Where $\alpha_4 = (C_{DS} + C_{OSS2} + C_{GD})(V_{GG(on)} - V_{th}) + I_L R_G C_{GD}$. $\beta_4 = -\tau_c G_m$. In (4), α_4 is positive whereas the ζ_4 is negative. For Si MOSFET, their G_m and V_{th} have NTCs. The impacts of dG_m/dT and dV_{th}/dT thereby counteract, which induces relatively weak temperature dependency of $dV_{DS}/dt|_{on}$. For SiC MOSFET, its G_m has a PTC and V_{th} has an NTC. The impacts of dG_m/dT and dV_{th}/dT add up, which induce a relatively large PTC for $dV_{DS}/dt|_{on}$. A strong temperature dependency on $dV_{DS}/dt|_{on}$ is thereby achieved for SiC MOSFET.

D. T_{J1} dependency of Turn-off dV/dt

1) IGBT: Temperature dependency of turn-off dV_{CE}/dt is:

$$\left.\frac{dV_{CE}^2}{dtdT}\right|_{off} = \frac{\alpha_5\dfrac{dG_m}{dT} + \beta_5\dfrac{dV_{th}}{dT} + \zeta_5\dfrac{dC_{ext}}{dT}}{\tau_d^2} \tag{5}$$

Where $\tau_d = C_{ext} + C_{CE} + C_{GC}(1+G_m R_G)$. $\alpha_5 = (C_{ext} + C_{CE} + C_{GC})(V_{th} - V_{GG(off)}) - C_{GC}R_G bI_L/(1+b)$. $\beta_5 = G_m\tau_d$. $\zeta_5 = -(G_m(V_{th} - V_{GG(off)}) + bI_L/(1+b))$. As shown in Fig. 2c, when the depletion region extends, the excess charge Q_t is extracted in the N-base, which generates a capacitive current. The equivalent capacitance C_{ext} is used to represent the capacitive behaviour [2], [9].

Compare to the V_{th} and G_m, the temperature dependency of C_{ext} is much stronger and thereby dominate the $dV_{CE}^2/dtdT|_{off}$[2], [6]. Since C_{ext} has a PTC, a NTC is obtained for $dV_{CE}/dt|_{off}$ due to the negative ζ_5.

2) Unipolar devices: Temperature dependency of turn-off dV_{ds}/dt of Si and SiC MOSFETs is [8]:

$$\left.\frac{dV_{DS}^2}{dtdT}\right|_{off} = \frac{\alpha_6\dfrac{dG_m}{dT} + \beta_6\dfrac{dV_{th}}{dT}}{\tau_e^2} \tag{6}$$

Where $\tau_e = C_{DS} + C_{OSS2} + C_{GD}(1+G_m R_G)$. $\alpha_6 = (C_{DS} + C_{OSS2} + C_{GD})(V_{th} - V_{GG(off)}) - I_L R_G C_{GD}$. $\beta_6 = \tau_e G_m$

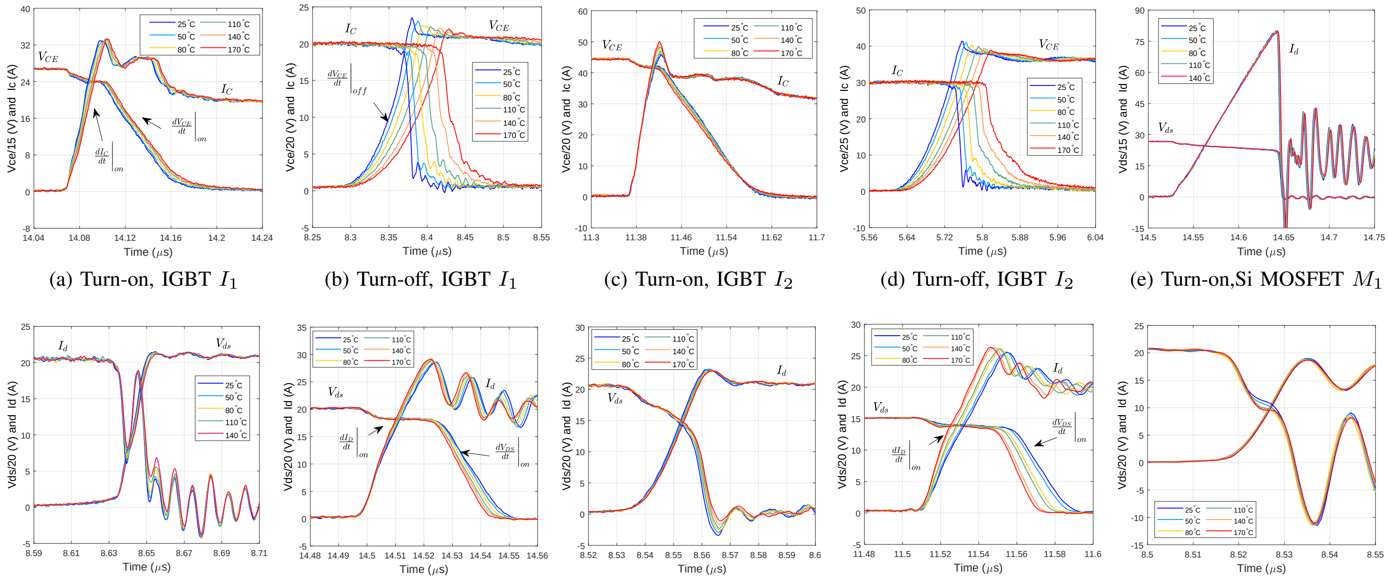

(a) Turn-on, IGBT I_1 (b) Turn-off, IGBT I_1 (c) Turn-on, IGBT I_2 (d) Turn-off, IGBT I_2 (e) Turn-on,Si MOSFET M_1

(f) Turn-off,Si MOSFET M_1 (g) Turn-on,SiC MOSFET S_1 (h) Turn-off,SiC MOSFET S_1 (i) Turn-on,SiC MOSFET S_2 (j) Turn-off,SiC MOSFET S_2

Fig. 3. Comparison of experimental switching waveforms when low-side T_{J1} varies while high-side $T_{J2} = 25°\text{C}$.

Noting that the β_6 is much larger than α_6 in the typical applications. The $dV_{DS}^2/dtdT|_{off}$ is thereby mainly determined by the dV_{th}/dT. For SiC MOSFET and Si MOSFET, their V_{th} have NTCs. Their turn-off $dV_{DS}/dt|_{off}$ thereby also have NTCs due to the positive β_6.

E. T_{J2} dependency of Turn-on dV/dt

The T_{J2} dependency of Turn-on dV/dt of IGBT, Si and SiC MOSFETs is:

$$\left.\frac{dV^2}{dtdT}\right|_{on} = -\frac{G_m(V_{GG(on)} - V_{th}) - I_L}{\tau_b^2}\frac{dC_{ext\_d}}{dT} \tag{7}$$

C_{ext_d} is the charge extraction capacitance induced by the excess charge dynamics in the N-base of the freewheeling diode, as shown in Fig. 2d. The C_{ext_d} is similar to that of C_{ext} for IGBT. When the junction temperature becomes higher , the excess charge Q_d greatly increases [10], which generates larger C_{ext_d}. The C_{ext_d} thereby has a PTC.

III. Experimental Investigation on Tmeperature Dependency of Switching Behaviour.

A. T_{J1} dependency on switching behaviour of IGBT, Si and SiC MOSFET

1) IGBT: Figs. 3a and c shows the turn-on waveforms of IGBTs I_1 and I_2 when T_{J1} is heated to various temperatures (from 25°C to 170°C) while T_{J2} is kept at 25°C. The $dI_C/dt|_{on}$ has a NTC for I_1 and PTC for I_2. According to (1), the dV_{th}/dT and dG_m/dT have opposite impacts on the $dI_C^2/dtdT|_{on}$, which give rise to weak T_{J1} dependency of $dI_C/dt|_{on}$.

In Figs. 3a and c, the temperature dependency of the $dV_{CE}/dt|_{on}$ agree with the analysis proposed for (3). In the beginning of V_{CE} falling transient, C_Q is approximately temperature-independent. The $dV_{CE}/dt|_{on}$ has a weak temperature dependency since the impacts of dV_{th}/dT and dG_m/dT counteract. When V_{CE} drops to tens of volts, C_Q becomes temperature-dependent, which induces an NTC for $dV_{CE}/dt|_{on}$. Fig. 3b and d compares the turn-off waveforms of f IGBTs I_1 and I_2 when T_{J1} varies from 25°C to 170°C while $T_{J2} = 25°\text{C}$. The $dV_{CE}/dt|_{off}$ greatly reduces with the increase of T_{J1} and has a NTC. The strong T_{J1} dependency is due to the temperature-dependent C_{ext} in (5).

Figs. 3b and d show the turn-off waveforms of I_C for IGBTs I_1 and I_2. In the initial I_C reduction phase, dI/dt slightly decreases with the increase of T_{J1} and has an NTC. In this phase, the current reduction is due to the MOS current turn-off. According to (2), the $dI^2/dtdT|_{off}$ is determined by dV_{th}/dT. Since the V_{th} of IGBT has an NTC, an NTC is thereby obtained for dI/dt in this phase. In Fig. 3b and d, the tail current greatly increases with the increase of T_{J1}. With higher T_{J1}, a higher excess carrier density is obtained, which generates a larger residual excess charge in the N-base to support tail current.

2) Si MOSFET: Fig. 3e compares the turn-on waveforms of Si MOSFET when T_{J1} varies from 25°C to 140°C, while T_{J2} is kept at 25°C. The $dI_D/dt|_{on}$ and $dV_{DS}/dt|_{on}$ of Si MOSFET decreases with when T_{J1} becomes higher and NTCs are obtained. In (1) and (4), the impacts of dV_{th}/dT and dG_m/dT counteract for both $dI^2/dtdT|_{on}$ and $dV_{DS}^2/dtdT|_{on}$. For the Si MOSFET, the dG_m/dT shows stronger impact and the a NTC is thereby obtained for $dI_D/dt|_{on}$ and $dV_{DS}/dt|_{on}$. However, the temperature dependency is very weak.

Fig. 3f compares the turn-off waveforms of Si MOSFET when T_{J1} varies from 25°C to 140°C while $T_{J2} = 25°\text{C}$. The $dI_D/dt|_{off}$ and $dV_{DS}/dt|_{off}$ reduces with the increase of T_{J1} and NTCs is obtained. Since $dI^2/dtdT|_{off}$ and

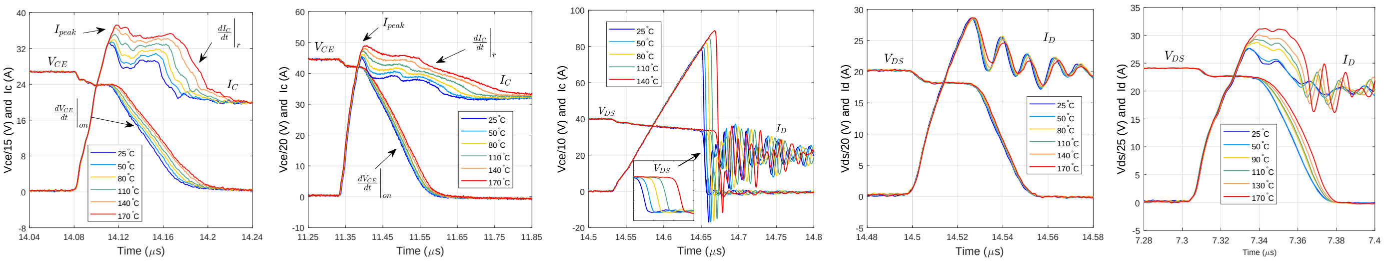

(a) IGBT I_1 (b) IGBT I_2 (c) Si MOSFET M_1 (d) SiC MOSFET S_1 (e) SiC MOSFET S_3

Fig. 4. Comparison of experimental turn-on waveforms when high-side T_{J2} varies while low-side $T_{J1} = 25°\text{C}$.

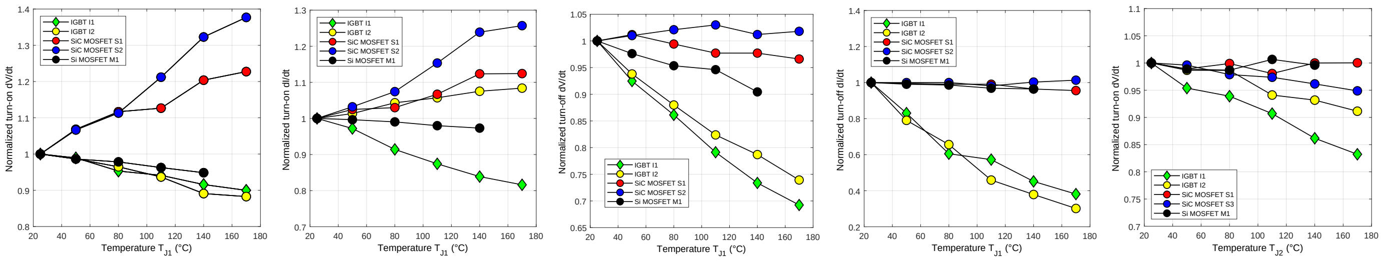

(a) (b) (c) (d) (e)

Fig. 5. Normalized dV/dt and dI/dt of IGBT, Si MOSFET and SiC MOSFET. (a) Normalized turn-on dV/dt, (b) Normalized turn-on dI/dt, (c) Normalized turn-off dV/dt, (d) Normalized turn-off dI/dt when T_{J1} varies while $T_{J2} = 25°\text{C}$. (e) Normalized turn-on dV/dt when T_{J2} varies while $T_{J1} = 25°\text{C}$.

$dV_{DS}^2/dtdT|_{off}$ are mainly determined by dV_{th}/dT, NTCs are thereby achieved for $dI_D/dt|_{off}$ and $dV_{DS}/dt|_{off}$.

3) SiC MOSFET: Figs. 3g and i compare the turn-on waveforms of SiC MOSFETs S_1 and S_2 when T_{J1} varies from 25°C to 170°C, while T_{J2} is kept at 25°C. Unlike the other devices, the $dI_D/dt|_{on}$ and $dV_{DS}/dt|_{on}$ of the SiC NOSFET increases when T_{J1} becomes higher. The PTCs of $dI_D/dt|_{on}$ and $dV_{DS}/dt|_{on}$ are due to the PTC of G_m. As shown in (1) and (4), with a PTC for G_m, the impact of dV_{th}/dT and dG_m/dT can add up. $dI_D/dt|_{on}$ and $dV_{DS}/dt|_{on}$ thereby have PTCs.

Figs. 3h and j compare the turn-off waveforms of SiC MOSFETs S_1 and S_2 when T_{J1} varies from 25°C to 170°C while $T_{J2} = 25°\text{C}$. With the increase of T_{J1}, $dI_D/dt|_{off}$ and $dV_{DS}/dt|_{off}$ reduces and have NTCs. As shown in (2) and (6), the $dV_{DS}^2/dtdT|_{off}$ and $dI^2/dtdT|_{off}$ of unipolar devices can be mainly determined by the dV_{th}/dT. Since V_{th} of S_1 has a NTC, $dI_D/dt|_{off}$ and $dV_{DS}/dt|_{off}$ for S_1 has a NTC, as shown in Fig. 3h. In (2) and (6), the impact of dV_{th}/dT and dG_m/dT can also contract with each other and $dI_D/dt|_{off}$ and $dV_{DS}/dt|_{off}$ of S_2 becomes temperature independent.

B. T_{J2} dependency on switching behaviour of IGBT, Si and SiC MOSFET

1) IGBT: Figs. 4a and b show the experimental turn-on waveforms of IGBTs I_1 and I_2 using various T_{J2}. With higher T_{J2}, the excess charge of p-i-n diode increases, which supports a higher peak current I_{peak}, softer reverse recovery and larger charge extraction capacitance C_{ext_d}. The I_{peak} thereby has a PTC whereas the $dV_{CE}/dt|_{on}$ have NTCs. In Figs. 4a and b, the snap-back current slop $dI/dt|_r$ also have NTC. This is

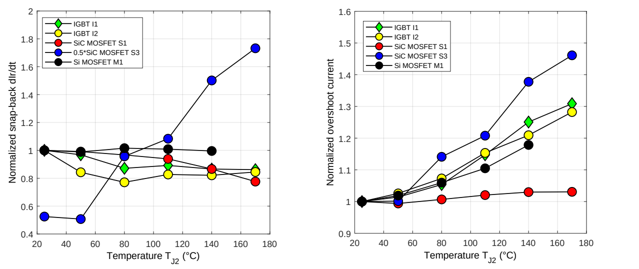

(a) (b)

Fig. 6. Normalized (a) dI_r/dt and (b) overshoot current I_o of IGBT, Si MOSFET and SiC MOSFET when T_{J2} varies while $T_{J1} = 25°\text{C}$.

because the higher temperature induced larger excess charge, which support softer reverse recovery.

2) Si MOSFET: Fig. 4c shows the turn-on waveforms of Si MOSFET M_1 utilizing various T_{J2}. With the increase of T_{J2}, a higher excess charge is used to support a larger I_{peak}. The I_{peak} thereby has PTC. In Fig. 4c, it can be noticed that the I_{peak} of Si MOSFET is very large. The large I_{peak} is due to the two-dimensional depletion behavior of superjunction, which exhausted the N-base excess charge to generates the large I_{peak} [11]. Since a very small amount of residual charge is left to support reverse recovery, high snap-back current slop $dI/dt|_r$ is generated [12]. Since the residual charge is negligible, the $dV_{DS}/dt|_{on}$ and $dI/dt|_r$ at turn-on are approximately temperature-independent.

3) SiC MOSFET: Figs. 4d and e shows the turn-on waveforms of SiC MOSFETs S_1 and S_3 using various T_{J2}. The peak current I_{peak} increase with the increase of T_{J2} and has PTC. The $dV_{DS}/dt|_{on}$ has a NTC and decreases when T_{J2}

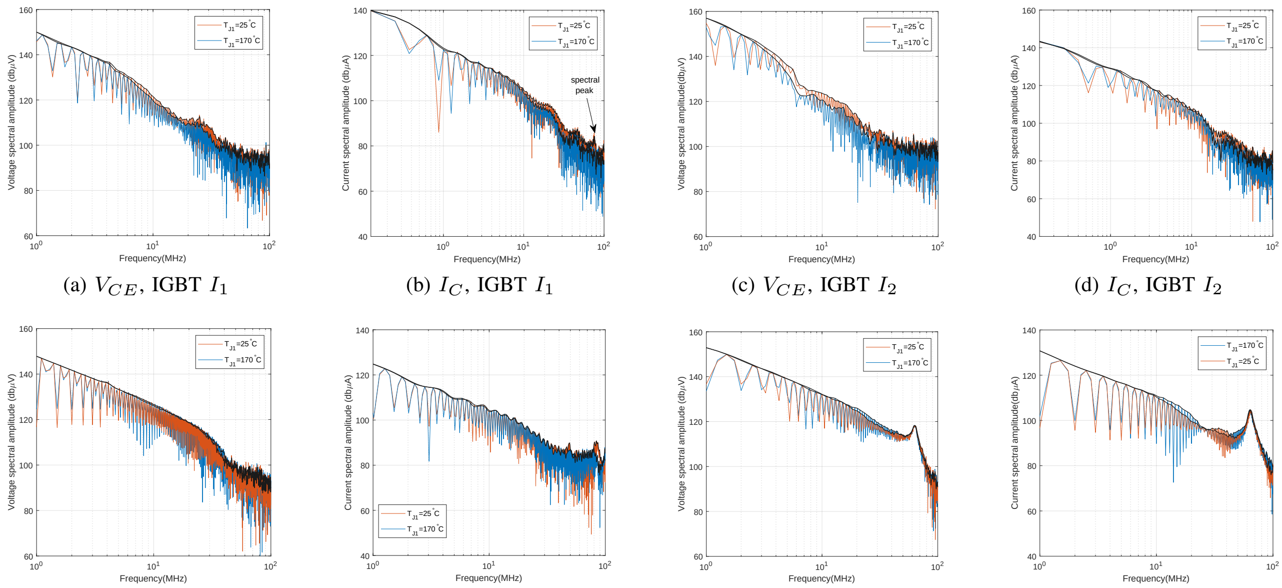

(a) V_{CE}, IGBT I_1 (b) I_C, IGBT I_1 (c) V_{CE}, IGBT I_2 (d) I_C, IGBT I_2

(e) V_{DS},SiC MOSFET S_1 (f) I_D,SiC MOSFET S_1 (g) V_{DS},SiC MOSFET S_2 (h) I_D,SiC MOSFET S_2

Fig. 7. Computed spectral amplitude of various devices when T_{J1} is 25°C and 170°C while $T_{J2} = 25$°C.

is higher. The $dI/dt|_r$ have NTC for S_1 and PTC for S_2.

IV. Comparison on T_{J1} and T_{J2} Dependency of Normalized dV/dt and dI/dt

Figs. 5a-d compare the T_{J1} dependent dV/dt and dI/dt for IGBTs, Si MOSFETs, SiC MOSFETs. In Figs. 5e and 6, the T_{J2} dependent turn-on dV/dt, overs shoot current I_{os} ($I_{os} = I_{peak} - I_L$) and $dI/dt|_r$ of IGBTs, Si MOSFETs, SiC MOSFETs are compared. Their values are extracted and normalized to their corresponding value at 25°C.

As shown in Figs. 5a and b, The SiC MOSFET S_1 and S_2 has large PTCs on turn-on dV/dt and dI/dt. When T_{J1} increases form 25°C 170°C, its turn-on dV/dt can increase upto 38% and turn-on dI/dt can increase upto 27%. The turn-on dV/dt of IGBTs has a relatively strong NTCs due to the temperature dependent C_Q. The turn-on dV/dt and dI/dt of Si MOSFET M_1 is the weakest.

As shown in Figs. 5c and d, the turn-off dV/dt and dI/dt of Si IGBT I_1 and I_2 shows the strongest T_{J1} dependency. This is because the turn-off behaviour of Si IGBT is greatly affected by the excess charge dynamic in the N-base. Due to the temperature dependent excess carrier density, the $dV_{CE}/dt|_{off}$ of IGBT shows strong T_{J1} dependency. Due to the unipolar nature, Si MOSFET and SiC MOSFET shows much weaker T_{J1} dependency on turn-off dV/dt and dI/dt.

As shown in Figs. 5e and 6, the IGBTs I_1 and I_2 and 1200V rated SiC MOSFET S_3 show strong T_{J2} dependency for turn-on dV/dt, I_{os} and $dI/dt|_r$. The S_3 also have strongest PTC of I_{os} and $dI/dt|_r$. This is due to the temperature-dependent excess charge in the N-base of the p-i-n diode. Moreover, the increase charge of S_3 is not able to support high I_{os}, which induces the large PTC of $dI/dt|_r$.

Due to the highly doped N-base, the 650V rated SiC MOSFET S_3 has a unipolar body diode and the T_{J2} dependency is very weak. With two-dimensional depletion behavior, the M_1 has strong T_{J2} dependency on I_{os}, while its turn-on dV/dt and $dI/dt|_r$ are temperature independent.

V. Temperature Dependency on EMI Generation

The switching waveforms of V_{CE} and I_C for IGBT are T_{J1} dependent. For SiC MOSFET, the T_{J1} has a significant impact on V_{DS} and I_D waveforms at turn-on transient. Following the approach presented in [5], [13], FFT is performed on the trapezoidal switching waveforms of IGBTs and SiC MOSFETs and Si MOSFET, which show strong temperature dependency.

A. T_{J1} dependent EMI of IGBT and SiC MOSFET

Figs. 7a-d show the FFT computed spectral amplitudes of V_{CE} and I_C when T_{J1} is 25°C and 170°C while $T_{J2} = 25$°C for IGBTs I_1 and I_2. The spectral envelopes are plotted in black lines. The V_{CE} spectral amplitude at $T_{J1} = 170°C$ reduces 2-5 dB within 4-80 MHz compared to that at $T_{J1} = 25°C$ due to the NTC $dV_{CE}/dt|_{off}$.

The I_C spectral amplitude at $T_{J1} = 170°C$ reduces 1-4 dB within 10-80 MHz compared to that at $T_{J1} = 25°C$. With higher T_{J1}, the $dI_C/dt|_{off}$ of IGBT greatly decreases, which gives rise to the reduction of I_C spectral amplitude.

Figs. 7e-h shows the FFT computed V_{DS} and I_D spectral amplitude for SiC MOSFETs S_1 and S_2 when T_{J1} is 25°C and 170°C while $T_{J2} = 25$°C. Since the turn-on dV/dt of SiC MOSFET has a PTC, V_{DS} spectral amplitude within 10-40 MHz increases 1-3 dB when T_{J1} varies from $25°C$ to $170°C$. Due to the PTC of turn-on dI/dt for SiC MOSFET, the I_D spectral amplitude at $T_{J1} = 170°C$ increases about 1-3 dB compared to that at $T_{J1} = 25°C$.

B. T_{J2} dependent EMI of IGBT, Si and SiC MOSFET

Figs. 8a show the FFT computed V_{CE} spectral amplitude of IGBT I_1 when T_{J2} is 25°C and 170°C while $T_{J1} = 25$°C. The

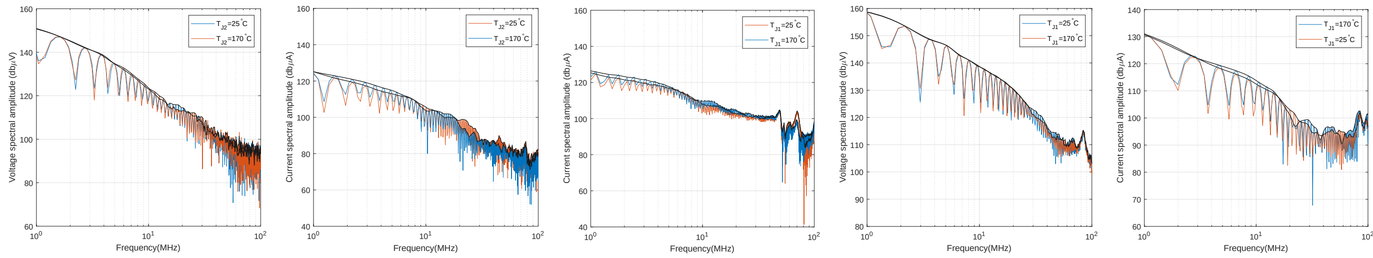

(a) V_{CE}, IGBT I_1 (b) I_C, IGBT I_1 (c) V_{DS},Si MOSFET M_1 (d) V_{DS},SiC MOSFET S_3 (e) I_D,SiC MOSFET S_3

Fig. 8. Computed spectral amplitude when T_{J2} is 25°C and 170°C while $T_{J1} = 25$°C.

spectral envelopes are plotted in black lines. Due to the NTC of turn-on dV/dt, the spectral amplitude of V_{CE} at $T_{J2} = 170°C$ within 14-20 MHz reduces 2-3 dB compared to that at $T_{J2} = 25°C$, as shown in Fig. 8a. Fig. 8b shows the FFT computed I_C spectral amplitude of IGBT I_1 when T_{J2} is 25°C and 170°C while $T_{J1} = 25$°C. Since the I_{os} of IGBT has a PTC while $dI/dt|_r$ has a NTC. Due to the PTC of I_{os}, the spectral amplitude of I_C at $T_{J2} = 170°C$ is 1-3 dB higher than that at $T_{J2} = 25°C$ within 12-20 MHZ. Due to the NTC of $dI/dt|_r$, the I_C spectral amplitude at $T_{J2} = 170°C$ reduces 1-6 dB within 20 - 50 MHZ compared to that at $T_{J2} = 25°C$.

Fig. 8c shows the I_D spectral amplitude of Si MOSFET M_1 when T_{J2} is 25°C and 140°C while $T_{J1} = 25$°C. Due to the PTC of I_{os} for Si MOSFET , the spectral amplitude of I_D at $T_{J2} = 140°C$ is 1-3 dB higher than that at $T_{J2} = 25°C$ within 1-40 MHz. Figs. 8 d-e show the I_D and V_{DS} spectral amplitude of SiC MOSFET S_3 when T_{J2} is 25°C and 170°C while $T_{J1} = 25$°C. Due to the NTC of turn-on dV/dt, the spectral amplitude of V_{DS} at $T_{J1} = 170°C$ becomes 1-4 dB lower than that at $T_{J1} = 25°C$ between 30-50 MHz. Due to the PTC of I_{os} and the high peak current indeuced snappy current overshot, the spectral amplitude of I_D at $T_{J1} = 170°C$ becomes 1-5 dB higher than that at $25°C$ between 15-90 MHz.

VI. Conclusion

This paper compares the impact of low-side T_{J1} and high-side T_{J2} on dV/dt and dI/dt and EMI generation for IGBTs, Si MOSFETs, and SiC MOSFETs. Due to the temperature dependency of excess charge dynamics in the N-base, the turn-on dV/dt, turn-off dI/dt and turn-off dV/dt of IGBT are strongly dependent on T_{J1} and have NTCs. Due to the NTC of G_m, the turn-on dI/dt of IGBT also has NTC, and its T_{J1} dependency is relatively strong. The current and voltage spectral amplitude of IGBT thereby reduce when T_{J1} increases. Since SiC MOSFET has a PTC for G_m, its temperature-dependent effects of G_m and V_{th} can add up at turn-on transient. This induces large PTCs of turn-on dI/dt and turn-on dV/dt, which generate the T_{J1} dependency of the current and voltage spectral amplitude for SiC MOSFET. The dV/dt and dI/dt of Si MOSFET have a weak T_{J1} dependency. In the end, the temperature-dependent EMI generation for IGBTs, Si MOSFETs and SiC MOSFETs are also clarified.

Acknowledgment

This work was supported by the CLEAN-Power (Compatibility and Low electromagnetic Emission Advancements for Next generation Power electronic systems) project at the Department of Energy, Aalborg University, Aalborg, Denmark, funded by Independent Research Fund Denmark (DFF)

References

[1] P. Xue and P. Davari, "A Temperature-Dependent dV_{CE}/dt and dI_C/dt Model for Field-Stop IGBT at Turn-on Transient," *IEEE Transactions on Power Electronics*, vol. 38, no. 6, pp. 7128–7141, 2023.

[2] P. Xue and P. Davari, "A Temperature-Dependent dV_{CE}/dt Model for Field-Stop IGBT at Turn-Off Transient," *IEEE Journal of Emerging and Selected Topics in Power Electronics*, vol. 11, no. 3, pp. 3173–3183, 2023.

[3] J. O. Gonzalez, O. Alatise, J. Hu, L. Ran, and P. A. Mawby, "An investigation of temperature-sensitive electrical parameters for sic power mosfets," *IEEE Transactions on Power Electronics*, vol. 32, no. 10, pp. 7954–7966, 2016.

[4] S. Jahdi, O. Alatise, P. Alexakis, L. Ran, and P. Mawby, "The impact of temperature and switching rate on the dynamic characteristics of silicon carbide Schottky barrier diodes and MOSFETs," *IEEE Transactions on Industrial Electronics*, vol. 62, no. 1, pp. 163–171, 2014.

[5] P. Xue and P. Davari, "The trade-off of switching losses and EMI generation for SiC MOSFET with common source and Kelvin source configurations," in *EPE'23 ECCE Europe*, IEEE, 2023, pp. 1–8.

[6] A. Bryant et al., "Investigation into igbt dv/dt during turn-off and its temperature dependence," *IEEE Transactions on Power Electronics*, vol. 26, no. 10, pp. 3019–3031, 2011.

[7] H. Li, X. Liao, Y. Hu, Z. Zeng, E. Song, and H. Xiao, "Analysis of SiC MOSFET dI/dt and its temperature dependence," *IET Power Electronics*, vol. 11, no. 3, pp. 491–500, 2018.

[8] P. Xue and P. Davari, "A Temperature-Dependent Analytical Transient Model of SiC MOSFET in Half-Bridge Circuits," *IEEE Transactions on Power Electronics*, vol. 40, no. 1, pp. 892–905, 2025.

[9] P. Xue and F. Iannuzzo, "Analytical Transient Model of Field-Stop IGBT Accounting for Temperature Dependence," *IEEE Transactions on Power Electronics*, 2025.

[10] H. Luo, Y. Chen, W. Li, and X. He, "Online high-power pin diode junction temperature extraction with reverse recovery fall storage charge," *IEEE Transactions on Power Electronics*, vol. 32, no. 4, pp. 2558–2567, 2016.

[11] P. Xue and G. Fu, "Analysis of the reverse recovery oscillation of superjunction mosfet body diode," *Solid-State Electronics*, vol. 129, pp. 81–87, 2017.

[12] P. Xue, L. Maresca, M. Riccio, G. Breglio, and A. Irace, "Investigation on the self-sustained oscillation of superjunction MOSFET intrinsic diode," *IEEE Transactions on Electron Devices*, vol. 66, no. 1, pp. 605–612, 2018.

[13] N. Oswald et al., "An experimental investigation of the tradeoff between switching losses and EMI generation with hard-switched all-Si, Si-SiC, and all-SiC device combinations," *IEEE Transactions on Power Electronics*, vol. 29, no. 5, pp. 2393–2407, 2013.